5-2024

The synthesis and characterization of 9,10-Bis-(iodoethynyl)anthracene for 2D molecular crystals from halogen-bonding

Nehemiah Antoine
University of Tennessee at Chattanooga, 20nantoine@gmail.com

THE SYNTHESIS AND CHARACTERIZATION OF 9,10-BIS-[IODOETHYNYL]ANTHRACENE FOR 2D MOLECULAR CRYSTALS FROM HALOGEN BONDING

Nehemiah Antoine

A Departmental Honors Thesis

The University of Tennessee at Chattanooga

Department of Chemistry and Physics

Examination Date: April 11, 2023

Keenan Dungey	Jared Pienkos
Department Head of Chemistry and Physics	Assistant Professor of Chemistry
Thesis Director	Department Examiner

Tom R. Rybolt

Assistant Professor of Chemistry

Department Examiner

Acknowledgments

I would like to thank everyone who has assisted me with this thesis and research:

Dr. Keenan Dungey, for helping me write this thesis and for assisting me with STM characterization.

Dr. Jared Pienkos, for helping write this thesis and for assisting me with synthesis and NMR characterization.

Dr. Tom Rybolt, for providing valuable advice for this research.

The University of Tennessee Department of Chemistry and Physics, for providing travel funding and for supporting this thesis and research.

Dr. Colin McMillen from Clemson University, for providing crystal structures and data

Mr. Richard X. Zhang, for providing the funding for this research through the Tom Rybolt and Richard X. Zhang Endowed Undergraduate Research in Chemistry Scholarship and for giving me an opportunity to spend a summer on this project.

Marisa James, for all the synthesis, recrystallization, and NMR characterization she did

Table of Contents

I. Abstract

Two-dimensional crystals have unique properties, giving them the potential to develop practical items such as electronics, biomedicine, and sensors. Our goal is to use chemical principles to synthesize molecules that spontaneously form 2D crystals with designed patterns and properties. For this, we will exploit directional, non-covalent interactions to determine what pattern will form in 2D. In this project halogen-bonding will be utilized: halogen-bonding is the interaction between the electrophilic region of a halogen and a nucleophilic region of a Lewis base. We are functionalizing anthracenes with iodine and nitrogen to form halogen bonds that enable the molecules to pack more uniformly. The flat, stable, conjugated composition of anthracenes makes them good candidates for 2D molecular crystals. Our hypothesis is that halogen-bonded anthracenes will have an offset row tiling pattern in 2D.

II. Introduction

Two-dimensional crystals have unique properties, giving them the potential to develop practical items such as electronics, biomedicine, and sensors.[1] Our goal is to use chemical principles to synthesize molecules that spontaneously form 2D crystals with designed patterns and properties. In addition to characterization techniques such as NMR spectroscopy and crystallography, scanning tunneling microscopy will be used to analyze these molecules. A scanning tunneling microscope (STM) can be used to view compounds at the nanometer scale using a phenomenon called quantum tunneling. Gerd Binning and Heinrich Rohrer invented the microscope in 1981, winning half of the Nobel Prize in Physics in 1986.[1] Micrographs made by an STM would ideally show a unique pattern formed by a compound's atomic bonding. Compounds must be flat, stable at room temperature, and have molecules that are oriented in an orderly array (called a 2D crystal) in order to be imaged by an STM.[2]

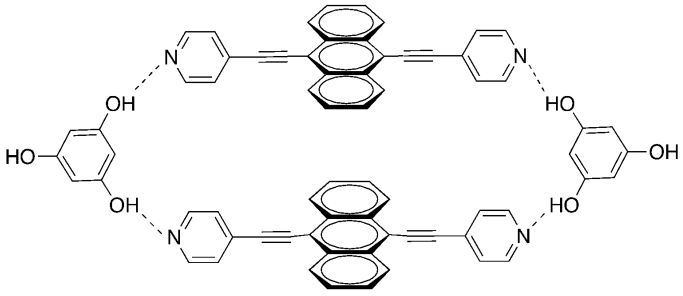

Figure 1. A depiction of 9,10-bis(4-pyridylethynyl)anthracene•1,3,5-tri(hydroxy)benzene. Hydrogen bonding (shown by the dotted lines) can be observed between the moieties.[3]

The flat, stable composition of anthracenes makes them good candidates for STM analysis. Prior studies illustrate the principles for forming 2D molecular crystals with anthracenes. Non-covalent interactions arrange adjacent molecules into desired orientations. Hydrogen bonding is a well-known example of such a directional, non-covalent attraction. The compound 9,10-bis(4-pyridylethynyl)anthracene formed a hydrogen-bonded 3D network with 1,3,5-tri(hydroxy)benzene, as shown in Figure 1.[3] The π-π interactions among adjacent

anthracene moieties provided extra structure to the network. In my study, hydrogen bonding will be replaced with halogen bonding, which is the interaction between the electrophilic region of a halogen and the nucleophilic region of a Lewis base.[4] For anthracenes to undergo halogen bonding, they need to be either a halogen bonding donor (have a substituent with a halogen) or a halogen bonding acceptor (have a substituent with a Lewis base). We functionalized anthracene with iodine, making it a halogen-bond donor (reaction schemes are shown in Figure 2). This would help it bond with pyrazine, a halogen-bond acceptor. Our eventual goal is to grow 2D crystals of the halogen-bonded complex onto a graphite surface and analyze them by STM. Our research question is: how does halogen bonding direct the 2D molecular crystal lattice of anthracenes? Our hypothesis is that halogen-bonded anthracenes would have an offset tile pattern as visualized by STM.

This thesis is structured into eight parts: the Abstract, Introduction, Background, Experimental Section, Results and Discussion section, Conclusions section, References section, and Appendix. The Abstract is a brief paragraph about the overview of this research and its expectations. The Introduction is a detailed version of the abstract that puts more emphasis on why and how certain things were done. The Background focuses on the fundamental ideas and concepts that our research is based upon, with reference to prior research and theory. The Experimental Section shows what materials and instrumentation were used to perform experiments and collect data, and states the procedures of each experiment. The Results and Discussion section shows NMR spectra and their analysis. The Conclusions section briefly summarizes the results and mentions future work on this research. The References section contains a list of citations that this thesis references, formatted in ACS style. The Appendix contains a crystal structure report based on the title compound.

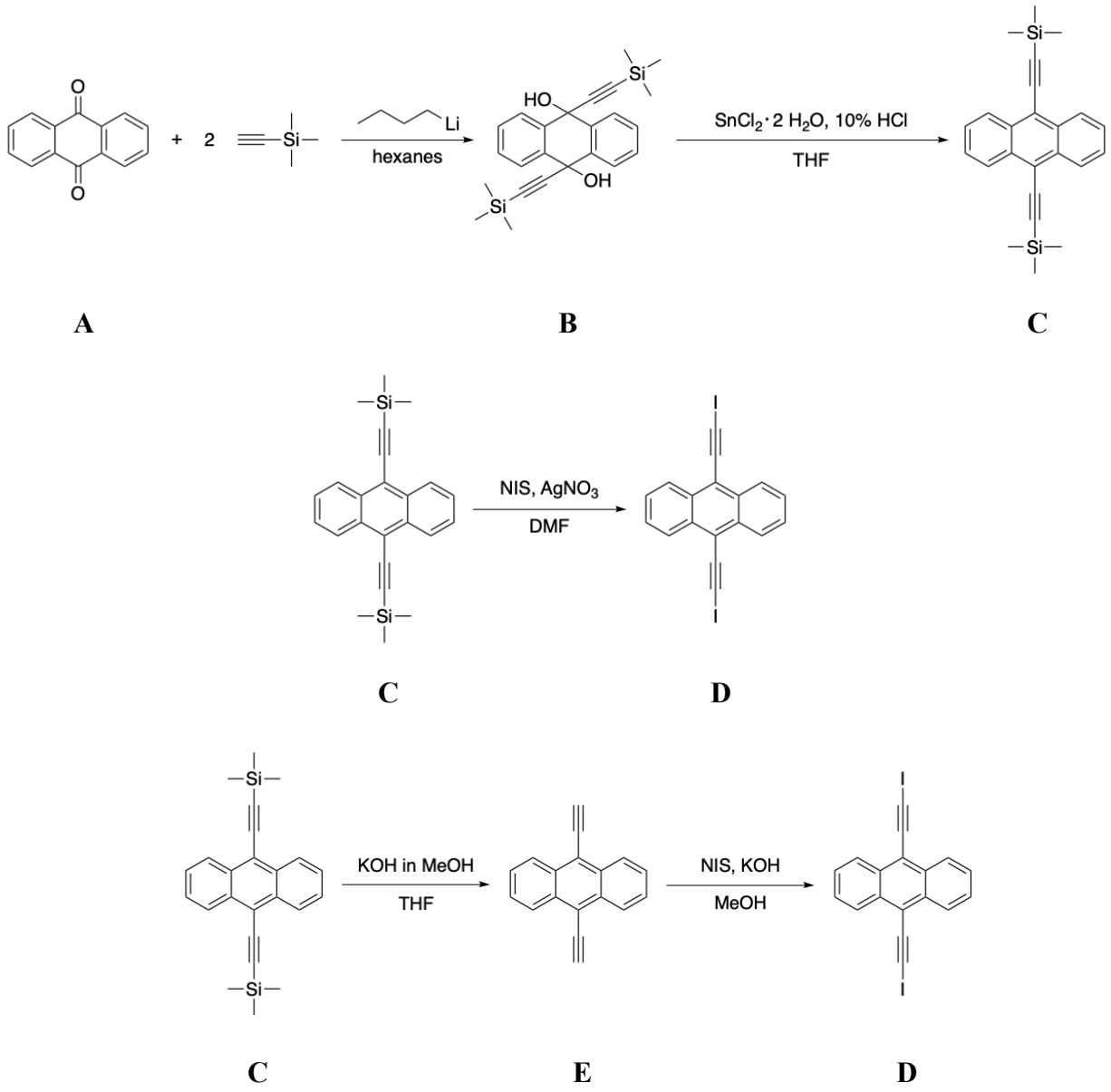

Figure 2. Reaction schemes for the synthesis of 9,10-bis(iodoethynyl)anthracene. Molecules are labeled for context for the Experimental Section.

III. Background

The scanning tunneling microscope (STM) is part of a family of instruments called scanning probe microscopes (SPMs) that are used in surface analysis and molecular characterization. The microscope was created in 1981 by Gerd Binning and Heinrich Rohrer at the IBM Zurich research lab. The duo won half of the Nobel Prize in Physics in 1986. Their main objective for the instrument was to identify two things: single atoms on conductive surfaces and molecules adsorbed on those surfaces.[1] An STM brings an atomically sharp tip extremely close to a metal or semiconductive surface. The surface may or may not have molecules adsorbed to it. When a bias voltage is applied between the tip and the surface, electrons are induced to "jump" between the tip and the surface if they are close enough to each other (from a few to tens of angstroms apart). STMs use the principles of quantum tunneling to provide high resolution at the atomic scale.[2]

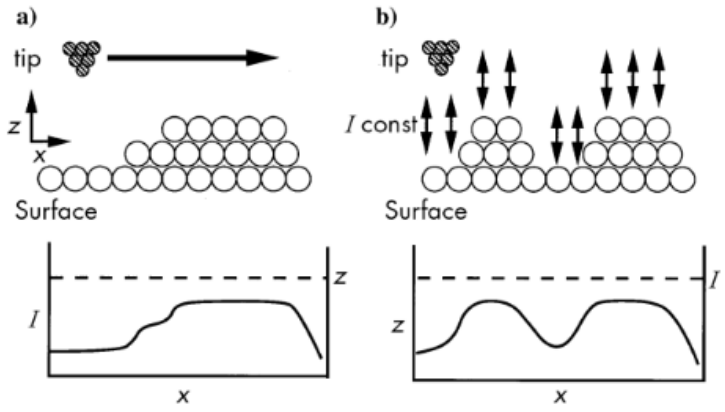

Figure 3. A diagram of the constant-height (a) and constant-current (b) modes of an STM.[2]

As shown in Figure 3, an STM has two distinct modes of operation: constant height and constant current. In the constant height mode (Figure 3a), the tip is positioned at a fixed distance *z* from the surface using a piezo ceramic element. As a voltage is applied, the tip scans across the sample, measuring tunneling current for the desired number of *x*, *y* positions. In the constant

current mode (Figure 3b), the tip is moved vertically (*z-direction*) to keep a fixed current when the piezo scans the tip across the sample. The height is measured and plotted at every *x*, *y* position in order to give a topographic map of the sample. The "bright" spots that appear on an STM micrograph correspond to regions of the sample that are topographically high (protrusions). In contrast, "dark" spots represent regions that are topographically low (depressions). Geometric-topographic and electronic coupling effects can also be responsible for increased brightness. A correlation that helps with distinguishing functional groups when analyzing STM micrographs is that brightness has a direct relationship with molecular polarizability. For example, a chlorine atom would appear "brighter" than a fluorine atom but "darker" than a bromine atom.[2]

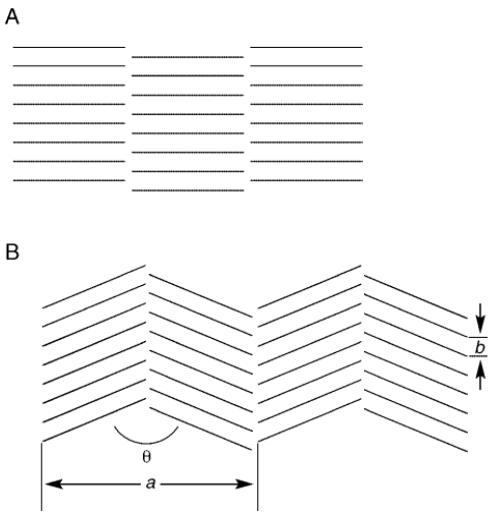

Figure 4. A diagram of STM patterns for unsubstituted alkanes (A) and substituted alkanes (B).[5]

Intermolecular forces, also known as non-covalent interactions, play a significant role in how patterns appear on STM micrographs. When molecules arrange themselves to form a 2D crystal, they display a unique pattern that reflects their orientation with each other. Weak intermolecular forces, such as van der Waals forces, can form simple, parallel patterns (Figure 4a). Unsubstituted alkanes (like long-chain hydrocarbons) show this patterning since they are

non-polar and do not have functional groups that would encourage stronger interactions. Conversely, substituted alkanes disturb van der Waals forces, resulting in a more complex pattern. With their functional groups, stronger intermolecular forces such as dipole-dipole interactions and hydrogen bonding can occur. For instance, hydrogen bonding occurs with alcohols since they have a hydroxyl functional group, yielding a herringbone pattern (Figure 4b) on their STM micrographs.[5]

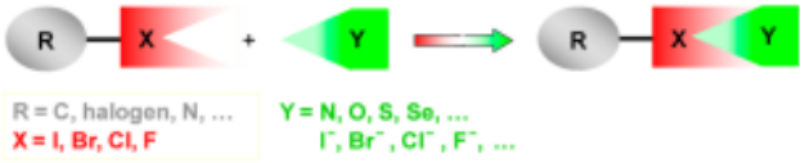

Figure 5. A schematic of the components of a halogen bond and what elements satisfy them. X is the halogen-bond donor and Y is the halogen-bond acceptor.[4]

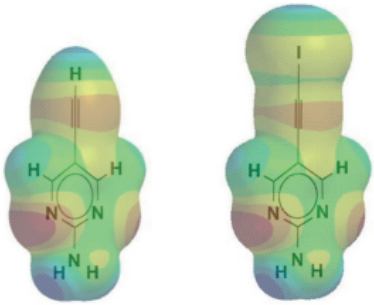

Figure 6. Electrostatic potential maps of 5-ethynyl-2-aminopyrimidine (left) and 5-iodoethynyl-2-aminopyrimidine (right). Unlike hydrogen, iodine has an area of high electron density of its own.[6]

The intermolecular force of interest for our research is halogen bonding, which is the interaction between the electrophilic region of a halogen and a nucleophilic region of a Lewis base. The molecule with the halogen that is involved in the interaction is called the "halogen-bond donor", and the Lewis base is called the "halogen-bond acceptor". The halogen participating in a halogen bond can be fluorine, chlorine, bromine, or iodine. The halogen-bond

acceptor can have atoms or regions of high electronegativity such as nitrogen, oxygen, sulfur, alkynyl groups, and halide ions (like Br^- and I^-). Figure 5 shows all the elements that could satisfy three components of a halogen bond: the halogen *X* involved in the halogen bond, the atom *Y* from the Lewis base that is involved in the bond, and the moiety *R* that is covalently bonded to the halogen in the halogen-bond donor.[4] In order to strengthen a halogen bond, the halogen participating in the bond must be polarized. Larger halogens such as iodine (which is the most commonly used) are easier to polarize than smaller halogens since they have high electron densities. Figure 6 has an electrostatic potential map that compares iodine's polarizability to hydrogen's. Unlike hydrogen, iodine has its own yellow band, which signifies a region of high electron density that can be polarized. The localization of electrons to a specific area of the iodine atom allows for electron-poor sites to form in other regions of the atom.[6] Interestingly, both the electron-rich and poor sites can be used for halogen bonding: the electron-poor site can be a halogen-bond donor and the electron-rich site can be a halogen-bond acceptor (Figure 7).[4] For example, prior studies show that triiodide can undergo halogen bonding with diiodotetrafluorobenzenes. An iodine on the triiodide can be the halogen-bond donor and the iodine on the diiodotetrafluorobenzene can be a halogen-bond acceptor, and vice versa.[7] In order for a halogen to be polarized, either the group that is covalently bonded to the halogen or the Lewis base that is halogen bonded to the halogen must have relatively high electronegativity. These nucleophiles induce a sigma hole (electron-poor site) in the adjacent halogen. Halogen bonds are commonly made with nitrogen as the atom for the Lewis base and alkynyl groups as the moiety covalently bonded to the halogen since both polarize halogens very efficiently due to their high electronegativities and electron densities.[4]

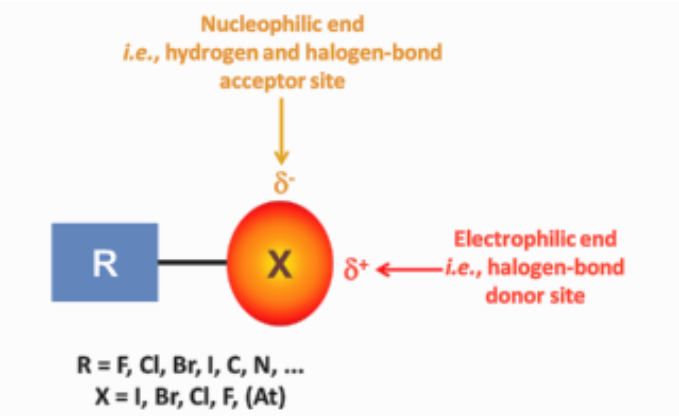

Figure 7. A diagram showing the locations of a halogen atom's halogen-bond donor and acceptor sites.[4]

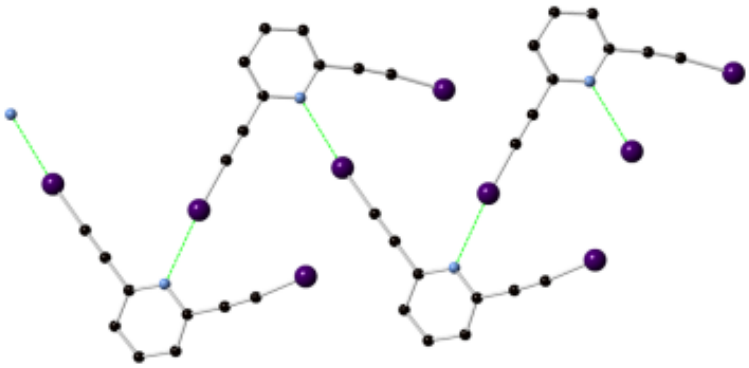

Figure 8. Crystal structure of 2,6-bis[iodoethynyl]pyridine. Halogen bonding (shown in green) can be observed between iodine and nitrogen atoms on adjacent molecules.[8]

Prior studies illustrate the synthesis and crystal structure analysis of molecules that form halogen bonds. The preparation of the crystals of 2,6-bis[iodoethynyl]pyridine (Figure 8) involved the gradual evaporation and cooling of a hot ethyl acetate solution, which yielded colorless crystals after several hours. Many other crystals were prepared in this way, including 5-iodoethynyl-2-aminopyrimidine (Figure 9) and 2,6-bis[iodoethynyl]pyridine with bromide (Figure 10, left image) and chloride (Figure 10, right image). X-ray diffraction was a common technique to characterize these molecules from imaging synthesized crystals. Crystal structures

were used to identify and analyze halogen bonds quantitatively. Figure 8 shows typical halogen bonding between iodine, the halogen-bond donor, and nitrogen, the halogen-bond acceptor.[8] Usually, iodine is expected to halogen bond to atoms on a Lewis base (like nitrogen), but it can also bond with alkynyl groups on adjacent halogen-bond donors and even other halogens. Figure 9 shows iodine halogen bonding to an ethynyl group, which serves as a halogen-bond acceptor due to its high electron density.[6] Figure 10 shows iodine halogen bonding to the halides bromide and chloride, which serve as halogen-bond acceptors due to their ability to be polarized. The electrons of those halides have an electrostatic attraction to the electropositive region of the iodine atom, causing an induced dipole within the halides.[8] Crystal structures help us determine and predict what kinds of halogen bonding can occur between molecules.

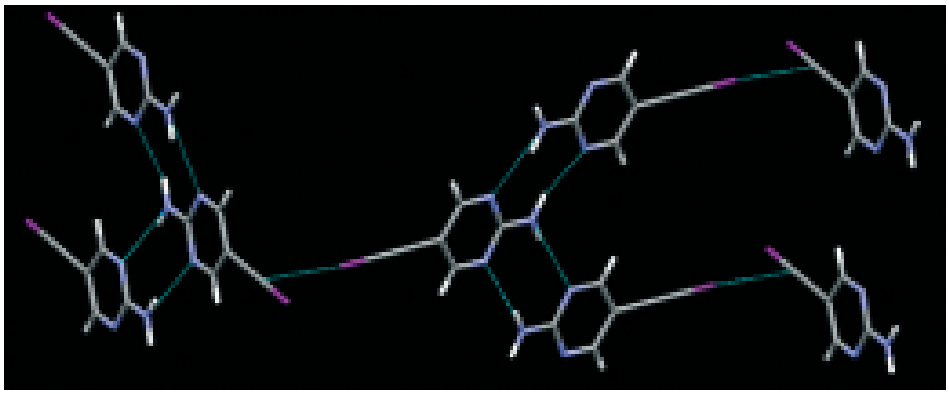

Figure 9. Crystal structure of 5-iodoethynyl-2-aminopyrimidine. Halogen bonding and hydrogen bonding (shown in teal) can be observed between iodine atoms and ethynyl groups on adjacent molecules.[6]

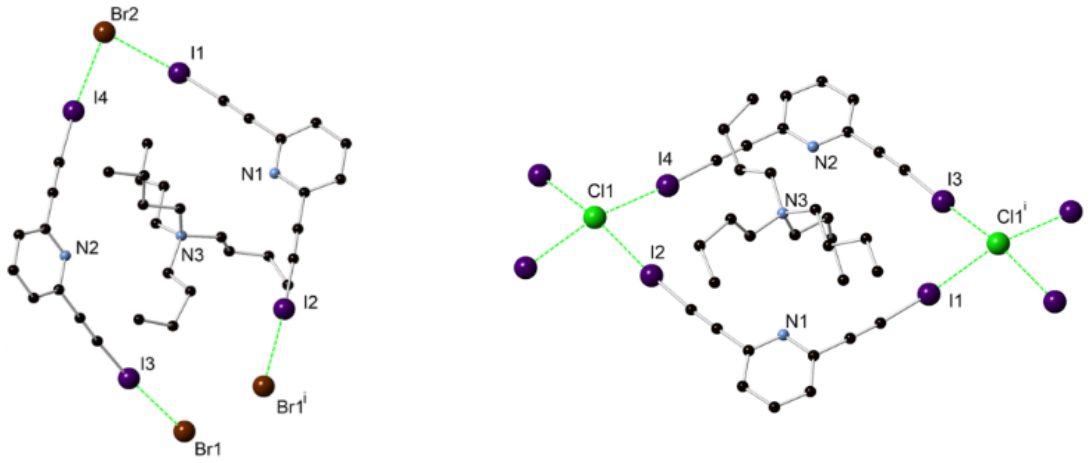

Figure 10. Crystal structures of 2,6-bis[iodoethynyl]pyridine with bromide (left) and chloride (right). Halogen bonding (shown in green) can be observed between iodine atoms and bromide or chloride.[8]

In order for compounds in a 2D array to be imaged by an STM, they have to be adsorbed onto a flat, stable, and unreactive surface. The surface should not react with the compound, therefore the compound too must be stable and unreactive as well. Graphite is a highly favored option for the job since it is electrically conductive and atomically flat, making it easier to work with in contrast to other compounds. Additionally, graphite's simple pattern scheme does not interfere with the pattern of the compound that is adsorbed on it. Even though graphite has a hexagonal pattern between its carbon atoms, a trigonal pattern (Figure 11) appears on their STM micrographs (every other carbon is "missing" due to differences in electron densities).[2]

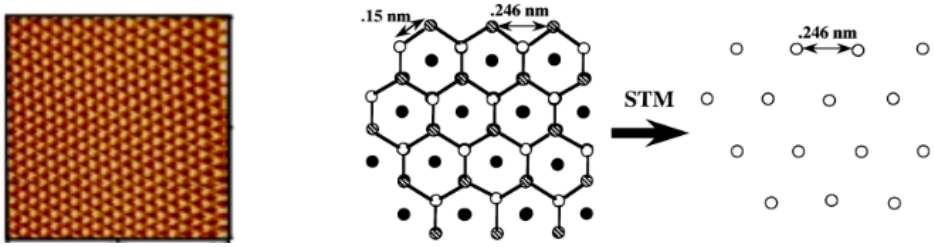

Figure 11. An STM micrograph of graphite (left) and a diagram comparing graphite's hexagonal pattern with its trigonal pattern (right).[2]

Prior studies illustrate the STM characterization and analysis of 2D crystals. Two compounds that were studied are 11-bromo-1-undecanol and n-decanol. The STM micrograph of 11-bromo-1- undecanol (Figure 12, left image) has a pattern of wide dim regions and short bright regions. The bright regions are formed by the electron-dense bromine atoms located at one of the ends of the 11-bromo-1-undecanol molecules. The dim regions represent the hydrocarbon chains and hydroxyl groups.[2] The STM micrograph of n-decanol (Figure 12, right image) has the pattern of a wave-like structure, with the brightest regions being at top of the "waves" and the darkest regions at the troughs. The brightest regions are formed by the hydroxyl groups located at the ends of the n-decanol molecules. The dim regions represent the hydrocarbon chains.[5] Both 11-bromo-1-undecanol and n-decanol use hydrogen bonding as the force that keeps their molecules together, thus forming 2D crystalline structures. Their herringbone pattern, as shown on their STM micrographs, can be attributed to the fact that they are substituted alkanes, as represented in Figure 4B.

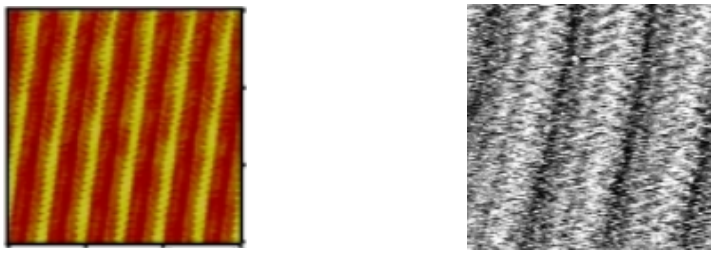

Figure 12. STM micrographs of 11-bromo-1-undecanol (left)[2] and n-decanol (right)[5].

Since molecules in a 2D crystal bond in certain ways, specific patterns would be formed based on their connectivities. Patterns that 2D crystals can make include hexagonal, square, rectangular, rhombus-centered rectangular, and parallelogram. Hexagonal patterns are the most common in STM micrographs. Figure 13 shows micrographs of each type of pattern.[9] Our hypothesis states that halogen-bonded anthracenes may have an offset row-tiling pattern, which is a type of rectangular pattern. 9,10-bis(iodoethynyl)anthracene, our compound of interest, can

halogen bond with pyrazine, in a linear fashion (Figure 14, left). Groups of this compound and pyrazine could be oriented anti-parallel to each other, forming the predicted offset row-tiling pattern (Figure 14, right).

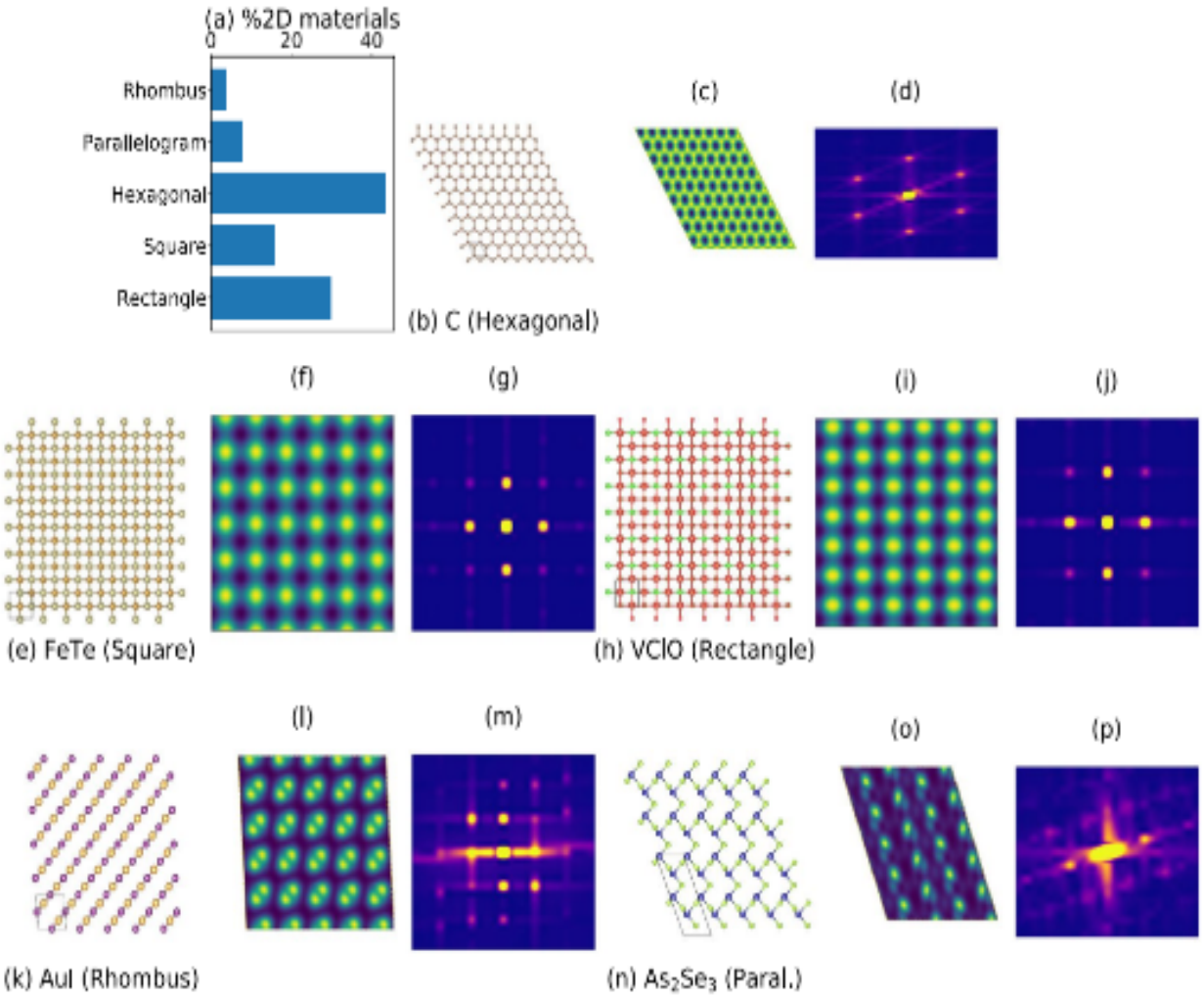

Figure 13. STM diagrams and micrographs show five types of patterns that 2D molecular crystals can form.[9]

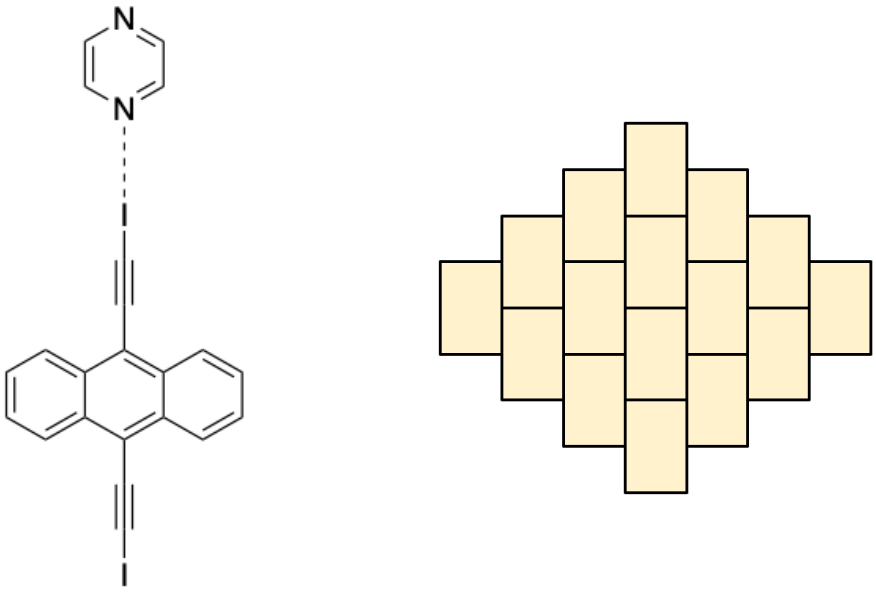

Figure 14. Predicted halogen bonding of 9,10-bis(iodoethynyl)anthracene with pyrazine (left) and a depiction of an offset row-tiling pattern (right). Halogen bonds are shown as dotted lines.*

IV. Experimental Procedures

Materials

Commercial reagents were purchased from Sigma Aldrich, Oakwood Chemicals, J.T. Baker, Fischer Chemical, and Thermo Scientific and used as received with the following exceptions: n-butyllithium was purged under nitrogen gas before its addition to a reaction mixture, and dimethylformamide was dried with molecular sieves prior to a reaction. All glassware was oven dried and cooled under a stream of nitrogen gas.

Instrumentation

Proton nuclear magnetic resonance (^{1}H NMR) spectra were obtained from a JEOL 400 MHz Fourier Transform NMR spectrometer. Single crystal X-ray diffraction data were collected at 100 K using a Bruker D8 Venture diffractometer with Mo K_α radiation (λ = 0.71073 Å) from a microfocus source, and a Photon 2 detector. The structure was resolved for a monoclinic cell with an F^2 of 1.131.

Synthesis of 9,10-dihydro-9,10-bis [2-(trimethylsilyl)ethynyl]anthracenediol

Added 10 mL of hexanes to trimethylsilylacetylene (0.831 mL, 3 equiv) in a round-bottomed flask. Stirred the reaction mixture while submerging the flask into an ice bath. The mixture was colorless and homogeneous. Added n-butyllithium (2 mL, 2.5 equiv) to the reaction mixture. The mixture became white and heterogeneous. Allowed the reaction to stir for 45 minutes and warm to room temperature. Added anthraquinone (**A**) (0.4168 g, 1 equiv) to the reaction mixture. The mixture became sandy brown and heterogeneous. Allowed the mixture to stir overnight.[10] Removed the solvent *in vacuo*. Dried the solid in a high vacuum. Isolated product in 77.53 % yield. The resulting solid, 9,10-dihydro- 9,10-bis[2- (trimethylsilyl)ethynyl] anthracenediol (**B**), was bony white and flaky.^{1}H NMR (400 MHz, Chloroform-*d*) δ 8.27 (m, 4H), 8.09 (m, 4H), 7.74 (ddd, J = 7.9, 7.3, 1.5 Hz, 4H), 7.56 (m, 4H), 4.73 (s, 2H), 0.17 (s, 18H).

Synthesis of 9,10-bis[2-(trimethylsilyl)ethynyl]anthracene

Dissolved **B** (0.4168 g, 1 equiv) in 5 mL of tetrahydrofuran using a round-bottomed flask. Purged the flask under nitrogen gas. The mixture was red and heterogeneous. Added tin (II) chloride dihydrate (1.793 g, 5 equiv) to the reaction mixture. The mixture became yellow and heterogeneous. Added 1 mL of 10% hydrochloric acid. Allowed mixture to stir for 30 minutes. The mixture became orange-brown and heterogeneous. Extracted reaction mixture with dichloromethane (3 x 20 mL).[10] Removed the solvent *in vacuo*. Dried the solid in a high vacuum. Used column chromatography to purify the product. Used flash column chromatography that was loaded with hexanes to collect product. The product had an R_f value of 0.475. Isolated product in 40.7 % yield. The resulting solid, 9,10-bis[2-(trimethylsilyl) ethynyl]anthracene (**C**), was orange and powdery. ^{1}H NMR (400 MHz, Chloroform-*d*) δ 8.57 (dd, J = 6.7, 3.3 Hz, 4H), 7.60 (m, 4H), 0.43 (s, 18H).

Synthesis of 9,10-[iodoethynyl]anthracene with $AgNO_3$

Added **C** (0.100 g, 1 equiv), *n*-iodosuccinimide (0.152 g, 2.5 equiv), silver nitrate (0.0069 g, 0.15 equiv), and 5 mL of dry dimethylformamide to a round-bottomed flask. Wrapped the flask with aluminum foil. The mixture was orange and heterogeneous. Allowed the reaction to stir for 6 hours. Used thin-layer chromatography to monitor the reaction's progress. Extracted reaction mixture with dichloromethane (30 mL) and washed it with deionized water (5 x 30 mL).[11] Removed the solvent *in vacuo*. Dried the solid in a high vacuum. One method of purification used was column chromatography. Used flash column chromatography that was loaded with hexanes, then 30 % ethyl acetate in hexanes to collect product. Used prep plate chromatography that was loaded with 30 % ethyl acetate in hexanes to collect product. The product had an R_f value of 0.400. Isolated product in 28.5 % yield. The resulting solid, 9,10-[iodoethynyl]anthracene (**D**), was red and chunky. ^{1}H NMR (400 MHz, Chloroform-*d*) δ 8.33 (d, J = 9.2 Hz, 4H), 7.82 (m, 4H).

Synthesis of 9,10-bis[ethynyl]anthracene

Dissolved **C** (0.285 g, 1 equiv) in 25 mL of tetrahydrofuran using a round-bottomed flask. The mixture was red-orange and homogeneous. Potassium hydroxide (0.216 g, 0.5 equiv) was dissolved in methanol (which was previously purged with nitrogen gas) and added to the reaction mixture. The mixture became yellow and heterogeneous. Allowed reaction mixture to stir for 4 hours, turning it orange and homogeneous.[12] Removed the solvent *in vacuo*. Dried the solid in a high vacuum. Used column chromatography to purify the product. Used flash column chromatography that was loaded with 30 % ethyl acetate in hexanes to collect product. The resulting solid, 9,10-bis[ethynyl]anthracene (**E**), was dark brown and chunky.

Synthesis of 9,10-bis[iodoethynyl]anthracene with KOH

Dissolved **E** (0.159 g, 1 equiv) in 8 mL of methanol using a round-bottomed flask that was submerged in an ice bath. The mixture was dark brown and heterogeneous. Allowed reaction mixture to stir for 10 minutes. Added potassium hydroxide (0.1970 g, 5 equiv) and *n*-iodosuccinimide (0.3799 g, 2.4 equiv). Allowed reaction mixture to stir for 15 minutes. Flask was taken out of the ice bath. Allowed reaction mixture to stir for an additional 20 minutes. The mixture became light brown and heterogeneous. Used thin-layer chromatography to monitor the reaction's progress. Extracted reaction mixture with diethyl ether (30 mL) and washed it with brine (3 x 30 mL).[13] Removed the solvent *in vacuo*. Dried the solid in a high vacuum. Used flash column chromatography that was loaded with hexanes, then 30 % ethyl acetate in hexanes to collect product. The resulting solid was orange and chunky. The compound was expected to be **D**, but NMR analysis confirmed it to be **C**.

Recrystallization of 9,10-[iodoethynyl]anthracene

Vapor-vapor diffusion was used for recrystallization. Small amounts of **D** were put into three glass tubes. Dichloromethane was pipetted into each tube until they were half full. Tubes were mixed until **D** completely dissolved, resulting in red, homogeneous solutions. The tubes were placed into a glass jar, which was filled halfway with hexanes. The amounts of dichloromethane and hexanes were in a 1:1 ratio. The jar was then screwed shut, wrapped in tape, and placed in a dark area for three days. The resulting crystals were red and needle-like.

V. Results and Discussion

^{1}H NMR analysis was used to confirm the purity and structure of Compounds **B**, **C**, and **D**. Each spectrum is accompanied by a tabulation and a closer view of the aromatic region.

Figure 15 contains the NMR spectrum of Compound **B**. There are four aromatic peaks (8.27 ppm, 8.09 ppm, 7.74 ppm, and 7.56 ppm) due to the cis/trans stereochemistry in **B**. The peak at 0.17 ppm represents the hydrogens in the trimethylsilane substituents. The peak at 4.73 ppm represents the hydrogens on the hydroxyl groups, a chemical shift that differs significantly from the literature (3.31 ppm)[14]. However, the frequencies of most other peaks relate quite well with those in the literature. The peaks at 8.09 ppm, 7.56 ppm, and 0.17 ppm correspond to the literature peaks at 8.05 ppm, 7.45 ppm, and 0.17 ppm,[14] respectively.

Figure 16 contains the NMR spectrum of Compound **C**. There is a reduction in peaks in the aromatic region (from four to two) since unlike **B**, **C** does not have a stereocenter, thus eliminating any possible stereochemical effects on the number of peaks that appear. The aromatic peaks are at 8.57 ppm and 7.60 ppm. The trimethylsilane peak moved downfield in **C**, from 0.17 ppm to 0.43 ppm, even though the hydroxyl group was removed. Fortunately, the peaks agree very well with those in the literature. The peaks at 8.57 ppm, 7.60 ppm, and 0.43 ppm correspond to the literature peaks at 8.58 ppm, 7.60 ppm, and 0.43 ppm,[14] respectively.

Figure 17 contains the NMR spectrum of Compound **D**, respectively. The aromatic peaks were shifted closer to each other in **D**, from 8.57 ppm and 7.60 ppm to 8.33 ppm and 7.82 ppm, respectively. Unlike **C**, **D** has a highly polarizable iodine atom. An induced dipole could form between the iodine and the electronegative ethynyl moiety that is covalently bonded to it. This electrostatic attraction can bring the electron density of the ethynyl groups more toward iodine and away from the anthracene. Therefore, the deshielding effect of the ethynyl group on the

anthracene protons decreases, which would lower the chemical shift. However, only one of the peaks shifts upfield. The protons associated with the peak shifting downfield could be affected by diamagnetic anisotropy, considering that the aromatic system of anthracene ends up having a greater effect on their shift than the ethynyl group.

Aside from NMR spectroscopy, Compound **D** was characterized and analyzed by crystallography. See the Appendix for the full crystal structure report, which contains an analysis of the crystal structure, tables of recorded crystallographic data, and figures that show the crystal structure of **D**.

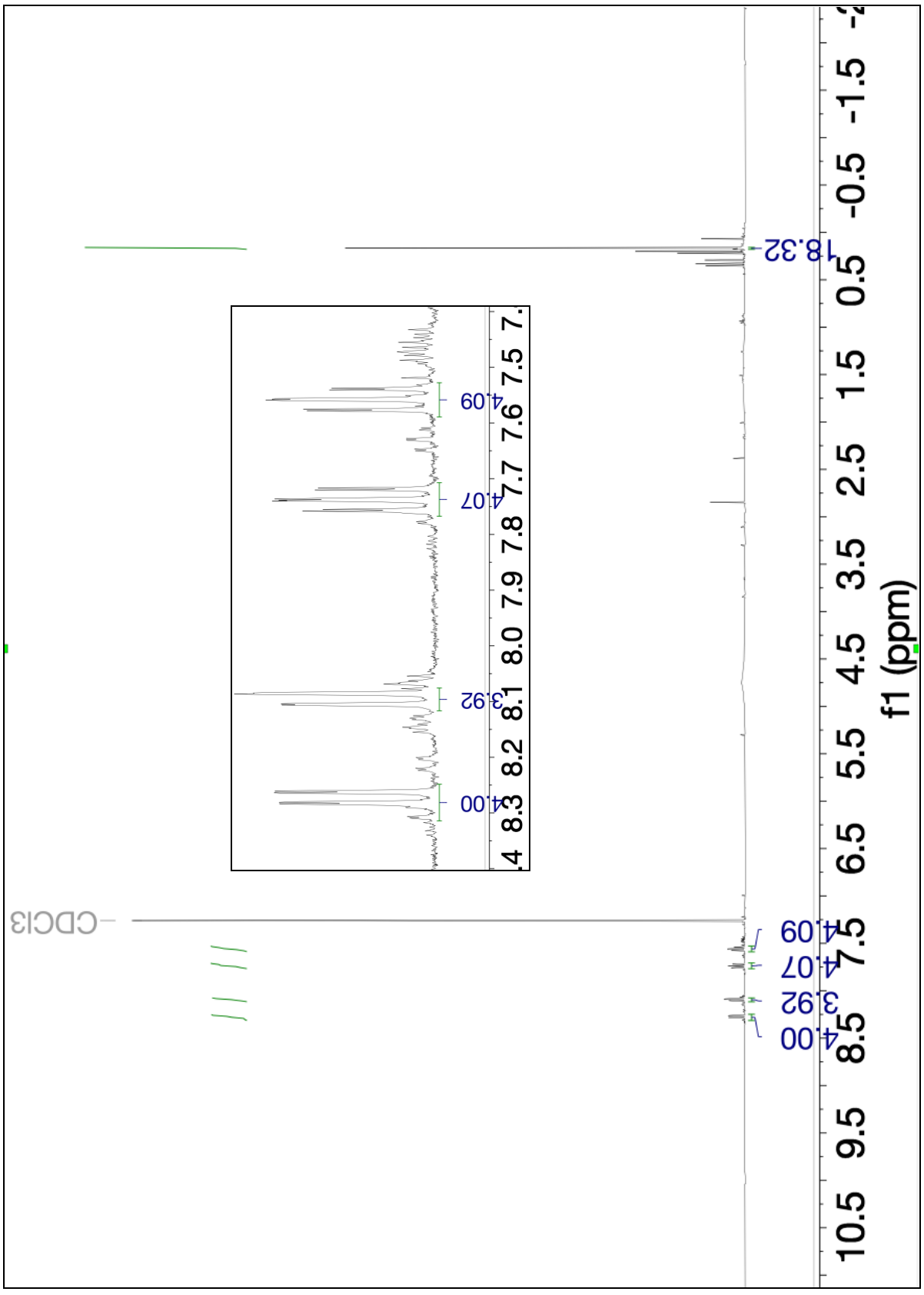

*Figure 15. ^{1}H NMR of 9,10-dihydro-9,10-bis[2-(trimethylsilyl)ethynyl]anthracenediol (**B**)*

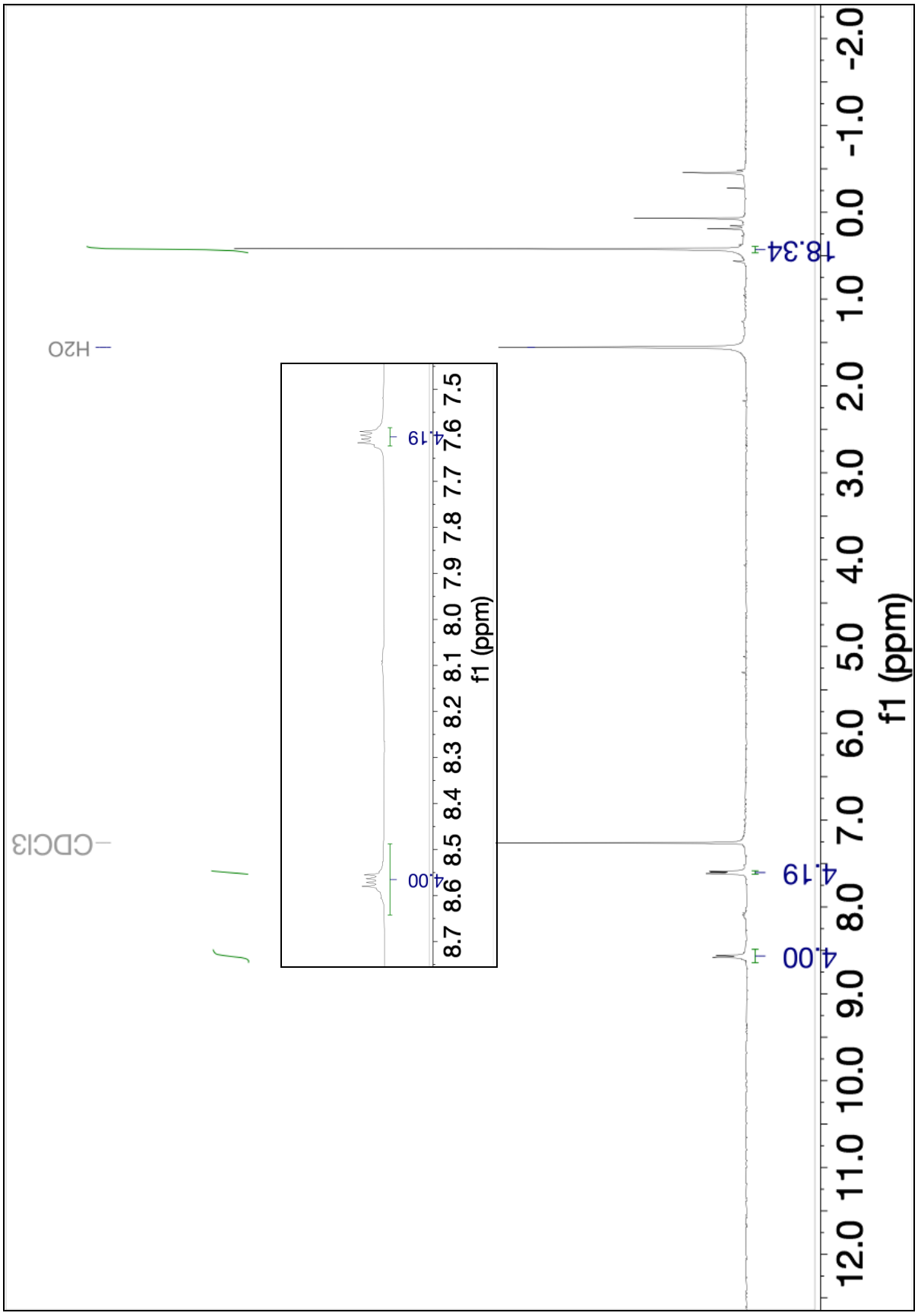

Figure 16. ^{1}H NMR of 9,10-bis[2-(trimethylsilyl)ethynyl]anthracene (C)

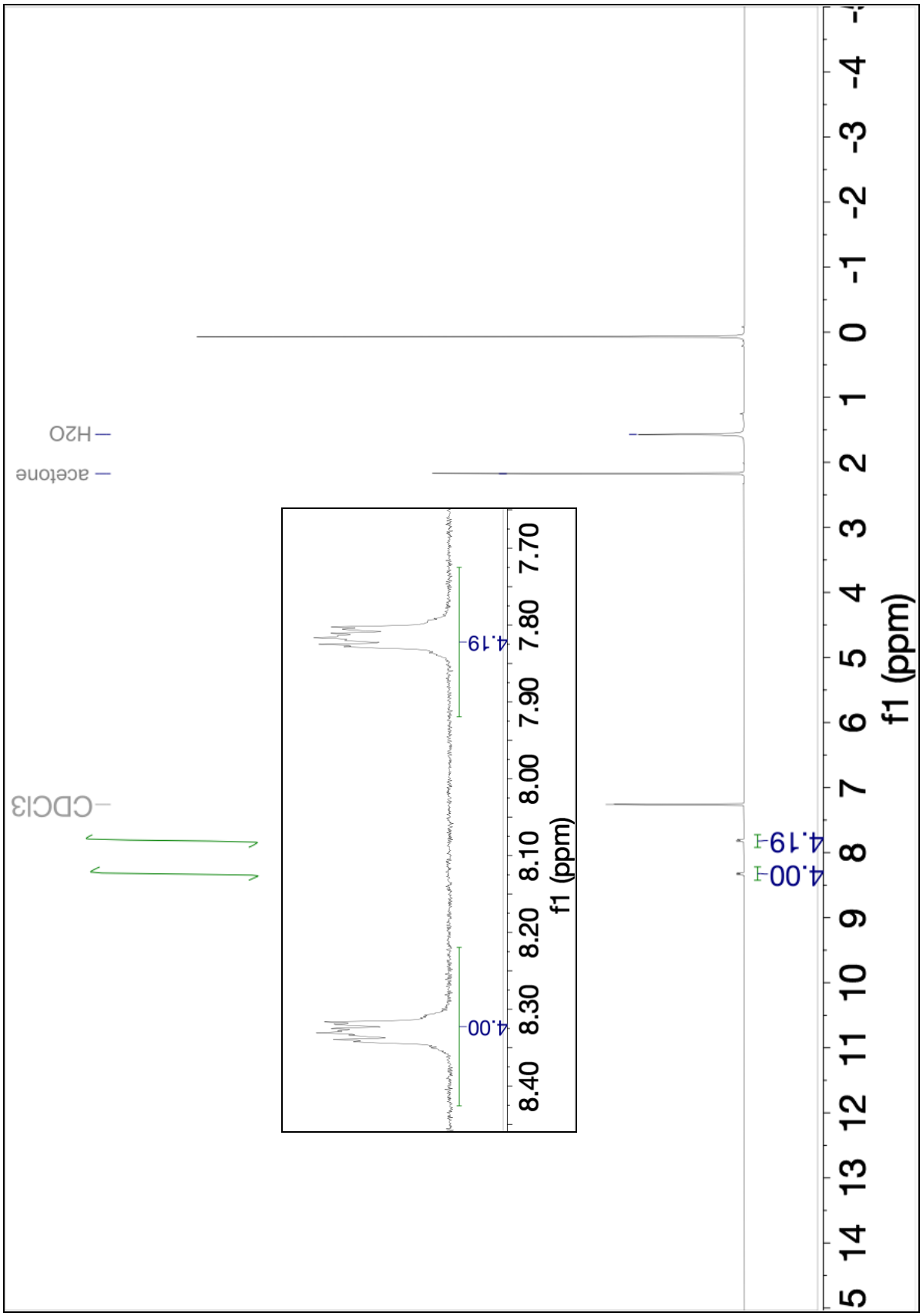

*Figure 17. ^{1}H NMR of 9,10-bis[iodoethynyl]anthracene (**D**)*

VI. Conclusions

We successfully synthesized and characterized the structure of 9,10-bis-(iodoethynyl) anthracene. The structure indicates π-π interactions are significant, with <4 Å spacing between molecules (C8-C1'). The herringbone stacking suggests halogen-π interactions, which is also indicated by the bent iodo-ethynyl bond (I-C-C angle of 177°). Future work involves obtaining the crystal structure of pyridine adducts and using the synthesized molecule for halogen bonding with pyridine derivatives. Scanning tunneling microscopy (STM) will be used to analyze the 2D crystal patterns formed by adducts of this compound with halogen-bond acceptors. Computational work will also be done on compound **D** to find out useful properties such as electrical potentials, molecular orbital structures, and bond energies.

VII. References

[1] Yan, X.; Zhao, Y.; Cao, G.; Li, X.; Gao, C.; Liu, L.; Ahmed, S.; Altaf, F.; Tan, H.; Ma, X.; Xie, Z.; Zhang, H. 2D Organic Materials: Status and Challenges. *Advanced Science* **2023**, *10* (7), 2203889.

[2] Giancarlo, L. C.; Fang, H.; Avila, L.; Fine, L. W.; Flynn, G. W. Molecular Photography in the Undergraduate Laboratory: Identification of Functional Groups Using Scanning Tunneling Microscopy. *Journal of Chemical Education* **2000**, *77* (1), 66.

[3] Tomislav, F.; MacGillivray, L.; Sokolov, A. Face-to-Face Stacking of Organic Semiconductor Building Blocks within Hydrogen-Bonded Molecular Cocrystals. *Journal of American Chemical Society* **2006,** *128*(9), 2806-2807.

[4] Cavallo, G.; Metrangolo, P.; Milani, R.; Pilati, T.; Priimagi, A.; Resnati, G.; Terraneo, G. The Halogen Bond. *Chemical Reviews* **2016**, *116* (4), 2478–2601.

[5] Pullman, D.; Peterson, K. I. Investigating Intermolecular Interactions via Scanning Tunneling Microscopy. an Experiment for the Physical Chemistry Laboratory. *Journal of Chemical Education* **2004**, *81* (4), 549.

[6] Aakeröy, C. B.; Welideniya, D.; Desper, J. Ethynyl Hydrogen Bonds and Iodoethynyl Halogen Bonds: A Case of Synthon Mimicry. *CrystEngComm* **2017**, *19* (1), 11–13.

[7] Kobra, K.; O'Donnell, S.; Ferrari, A.; McMillen, C. D.; Pennington, W. T. Halogen Bonding and Triiodide Asymmetry in Cocrystals of Triphenylmethylphosphonium Triiodide with Organoiodines. *New Journal of Chemistry* **2018**, *42* (13), 10518–10528.

[8] Barry, D. E.; Hawes, C. S.; Blasco, S.; Gunnlaugsson, T. Structure Direction, Solvent Effects, and Anion Influences in Halogen-Bonded Adducts of 2,6-Bis(Iodoethynyl)Pyridine. *Crystal Growth & Design* **2016**, *16* (9), 5194–5205.

[9] Choudhary, K.; Garrity, K. F.; Camp, C.; Kalinin, S. V.; Vasudevan, R.; Ziatdinov, M.; Tavazza, F. Computational Scanning Tunneling Microscope Image Database. *Scientific Data* **2021**, *8* (1).

[10] Petty II, A. J.; Odom, S. A. Ethynylated Acene Synthesis and Photophysics for an Organic Chemistry Laboratory Course. *Journal of Chemical Education* **2021**, *98* (5), 1741–1749.

[11] Tse, Y. C.; Docker, A.; Zhang, Z.; Beer, P. D. Lithium Halide Ion-Pair Recognition with Halogen Bonding and Chalcogen Bonding Heteroditopic Macrocycles. *Chemical Communications* **2021**, *57* (40), 4950–4953.

[12] Goudappagouda, G.; Wakchaure, V. C.; Ranjeesh, K. C.; Abhai, C. A.; Babu, S. S. Cascade Energy Transfer and Tunable Emission from Nanosheet Hybrids: Locating Acceptor Molecules through Chiral Doping. *Chemical Communications* **2017**, *53* (52), 7072–7075.

[13] Russo, M. V.; Lo Sterzo, C.; Franceschini, P.; Biagini, G.; Furlani, A. Synthesis of Highly Ethynylated Mono and Dinuclear Pt(II) Tethers Bearing the 4,4′-Bis(Ethynyl)Biphenyl (Debp) Unit as Central Core. *Journal of Organometallic Chemistry* **2001**, *619* (1-2), 49–61.

[14] Lydon, D. P.; Porrès, L.; Beeby, A.; Marder, T. B.; Low, P. J. A Simple “Palladium-Free” Synthesis of Phenyleneethynylene-Based Molecular Materials Revisited. *New Journal of Chemistry* **2005**, *29* (7), 972.

VIII. Appendix

Crystal Structure Report*

**To be Submitted to IUCr Data*

9,10-Bis-[iodoethynyl]anthracene

[a]Nehemiah Antoine; [a]Marisa James; [a]Keenan Dungey; [b]Colin McMillen; [a]Jared Pienkos

[a]Department of Chemistry and Physics, University of Tennessee at Chattanooga, Chattanooga, TN 37403, USA, and [b]Department of Chemistry, Clemson University, Clemson, SC 29634, USA

Correspondence Email: jared-pienkos@utc.edu

Keywords

crystal structure, 9,10-bis[iodoethynyl], anthracene, halogen bonding, pi-stacking

Synopsis

The title compound, 9,10-bis-[iodoethynyl]anthracene, is a substituted anthracene that exhibits halogen bonding.

Abstract

The substituted anthracene, 9,10-bis-[iodoethynyl]anthracene, contains bent I-C bonds on opposite sides of the anthracene. As a result of halogen bonding, the angles made from the carbons of each ethynyl group and iodine atoms slightly deviate from the expected 180°. π stacking also occurs between anthracene moieties.

Structure Description

Two-dimensional crystals have unique properties, giving them the potential to develop practical items such as electronics, biomedicine, and sensors.[4] Our goal is to use chemical principles to synthesize molecules that spontaneously form 2D crystals with designed patterns and properties. For this, we will exploit the directional, non-covalent interactions of halogen

bonding to determine what pattern will form in 2D. 9,10-bis-[iodoethynyl]anthracene is an anthracene that is functionalized with iodine to form halogen bonds that can enable uniform packing. The flat, stable, conjugated composition of anthracenes makes them good candidates for 2D molecular crystals.

The title compound, 9,10-bis-[iodoethynyl]anthracene (Figure 1), is an iodoethynyl-substituted anthracene that can participate in halogen bonding. On $C_{18}H_8I_2$, the I-C bonds, I1-C16 and I2-C18, both have a length of 1.996 (4) Å. These substituents are on opposite sides of the anthracene at the 9 and 10 positions and are *trans*- to each other. The angle that was expected from the sp carbons was 180°, but data shows the angles of C15-C16-I1 and C17-C18-I2 to be 177.4° (4) and 178.0° (3), respectively. The cause of this bending may be attributed to the I-π interactions between C(sp)-I and the π-electrons of the adjacent anthracene rings. This interaction can also be considered as halogen bonding, where iodine is a halogen-bond donor and the pi-bonds are halogen-bond acceptors. The halogen bonds, shown in Figure 2, have distances ranging from 3.352 Å to 3.655 Å. Since I1 has more halogen bonds than I2, C15-C16-I1 bends slightly more than C17-C18-I2. Related studies in the literature describe I-π interactions between C(sp)-I and π-electrons of ethynyl groups on adjacent molecules. For instance, 4-iodoethnynylanisole contains I-π halogen bonds with distances of 3.392 Å, similar to those of the title molecule.[2] Though I-π interactions decrease the stability of individual $C_{18}H_8I_2$ molecules by bending the C(sp)-I angle, they increase crystal stability as a whole due to more intermolecular interactions contributing to the lattice energy, in addition to π-π stacking (described below) and van der Waals forces.

In addition to the C(sp)-I···π interactions and bending of the C(sp)-I angle, anthracene portions of $C_{18}H_8I_2$ participate in π-π stacking. The molecules stack themselves in pairs, as shown

in Figure 3. C8-C1', which covers the distance between two anthracene carbons on adjacent molecules, has a length of only 3.969 Å. There are similar cases in the literature of π-π stacking occurring between anthracenes. For example, bis(2,4-dihydroxy-1-(hydroxy)-9,10-anthraquinonato)-copper(II) dihydrate has anthracenes with π-π stacking distances of 3.481 Å, which are about 0.5 Å closer than that of the title compound.[1] Besides I-π interactions, π-π stacking increases crystal stability due to the strengthening overlap of the aromatic p-orbitals. The planar structure of the anthracene allows for the aromatic moieties to easily stack close to each other.

Synthesis and Preparation

The following procedure was derived from that of 1,3-bis[(trimethylsilyl)ethynyl] -5-tertbutylbenzene.[3] Added 9,10-bis[trimethylsilyl]anthracene (0.100 g, 1 equiv), *n*-iodosuccinimide (0.152 g, 2.5 equiv), silver nitrate (0.0069 g, 0.15 equiv), and 5 mL of dry dimethylformamide to a round-bottomed flask. Wrapped the flask with aluminum foil. The mixture was orange and heterogeneous. Allowed the reaction to stir for 6 hours. Used thin-layer chromatography to monitor the reaction's progress. Extracted reaction mixture with dichloromethane (30 mL) and washed it with deionized water (5 x 30 mL). Removed the solvent *in vacuo*. Dried the solid in a high vacuum. One method of purification used was column chromatography. Used flash column chromatography that was loaded with hexanes, then 30 % ethyl acetate in hexanes to collect product. Used prep plate chromatography that was loaded with 30 % ethyl acetate in hexanes to collect product. The product had an R_f value of 0.400. Isolated product in 28.5 % yield. The resulting solid, 9,10-bis[iodoethynyl]anthracene, was red and chunky. ^{1}H NMR (400 MHz, Chloroform-*d*) δ 8.33 (d, *J* = 9.2 Hz, 4H), 7.82 (m, 4H).

Results

Table I: Crystal Data	
Chemical Formula	$C_{18}H_8I_2$
Formula Weight (g/mol)	478.04
Temperature (K)	100 (2)
Wavelength (Å)	0.71073
Crystal Size (mm)	0.131 x 0.145 x 0.171
Crystal System	monoclinic
Space Group	P 1 21/n 1
Unit Cell Dimensions: a, b, c (Å)	8.0022(3), 15.0735(7), 12.2506(5)
Volume ($Å^3$)	1468.83(11)
Z	4
Density (g/cm^3)	2.162
Absorption Coefficient (mm^{-1})	4.268
F(000)	888

Table II: Data Collection and Structure Refinement	
Theta Range for Data Collection	2.15 to 27.50°
Index Ranges	-10<=h<=10, -19<=k<=19, -15<=l<=15
Reflections Collected	37187
Independent Reflections	3373 [R(int) = 0.0365]
Max and Min Transmission	0.6050 and 0.5290
Structure Solution Technique	direct methods
Structure Solution Program	SHELXT 2018/2 (Sheldrick, 2018)
Refinement Method	Full-matrix least-squares on F^2
Refinement Program	SHELXL-2016/6 (Sheldrick, 2016)
Function Minimized	$\Sigma w(F_o^2 - F_c^2)^2$
Data / Restraints / Parameters	3373 / 0 / 181
Goodness-of-Fit on F^2	1.131
Δ/σ_{max}	0.001
Final R Indices	3084 data; I>2σ(I) R1 = 0.0263, wR2 = 0.0608
Weighting Scheme	$w = 1 / [\sigma^2(F_o^2) + (0.0142P)^2 + 7.1388P]$ where $P = (F_o^2 + 2F_c^2) / 3$
Largest Diff. Peak and Hole ($eÅ^{-3}$)	1.412 and -0.901
R.M.S. Deviation from the Mean ($eÅ^{-3}$)	0.120

Table III: Atomic Positions and Displacements									
Atom	x/a	y/b	z/c	U(eq)	Atom	x/a	y/b	z/c	U(eq)
I1	0.82384 (3)	0.70341 (2)	0.18275 (2)	0.02740 (8)	C14	0.3761 (5)	0.4645 (2)	0.2943 (3)	0.0190 (7)
I2	0.03465 (3)	0.12055 (2)	0.56404 (2)	0.02483 (8)	C15	0.6415 (5)	0.5464 (2)	0.2976 (3)	0.0201 (7)
C1	0.5433 (5)	0.4778 (2)	0.3413 (3)	0.0183 (7)	C16	0.7133 (5)	0.6047 (3)	0.2564 (3)	0.0226 (8)
C2	0.6141 (5)	0.4243 (2)	0.4292 (3)	0.0178 (7)	C13	0.3010 (5)	0.5178 (3)	0.2048 (3)	0.0234 (8)
C3	0.7841 (5)	0.4348 (3)	0.4760 (3)	0.0207 (7)	C17	0.2484 (5)	0.2737 (3)	0.4661 (3)	0.0224 (8)
C4	0.8486 (5)	0.3842 (3)	0.5624 (3)	0.0223 (8)	C18	0.1684 (5)	0.2157 (2)	0.5008 (3)	0.0227 (8)
C5	0.7470 (5)	0.3190 (3)	0.6078 (3)	0.0230 (8)	H3	0.8533	0.4778	0.4464	0.025
C6	0.5867 (5)	0.3059 (2)	0.5643 (3)	0.0196 (7)	H4	0.9620	0.3924	0.5928	0.027
C7	0.5139 (5)	0.3572 (2)	0.4729 (3)	0.0178 (7)	H5	0.7925	0.2846	0.6690	0.028
C8	0.3466 (5)	0.3430 (2)	0.4245 (3)	0.0190 (7)	H6	0.5209	0.2618	0.5948	0.024
C9	0.2770 (5)	0.3953 (2)	0.3353 (3)	0.0192 (7)	H10	0.0420	0.3373	0.3112	0.032
C10	0.1094 (5)	0.3826 (3)	0.2846 (3)	0.0266 (8)	H11	-0.0677	0.4241	0.1664	0.036
C11	0.0440 (5)	0.4340 (3)	0.1990 (4)	0.0297 (9)	H12	0.0948	0.5370	0.0987	0.034
C12	0.1413 (6)	0.5018 (3)	0.1588 (3)	0.0282 (9)	H13	0.3637	0.5648	0.1773	0.028

Table IV: Bond Lengths and Angles			
2-Atom Chain	Distance (Å)	3-Atom Chain	Angle (°)
C3-H3	0.950	I1-C16-C15	177.34
C3-C4	1.360	C16-C15-C1	175.42
C4-C5	1.427	C15-C1-C2	120.29
C1-C15	1.427	C4-C5-C6	120.32
C15-C16	1.192	H4-C4-C5	119.80
C16-I1	1.996		
I1-C2’	3.655		
I1-C6’	3.540		
I1-C7’	3.352		
I2-C13’	3.394		
I2-C14’	3.463		
C8-C1’	3.969		

Acknowledgments

We are grateful for the support of the UTC Irvine and Nita Grote Fund. Nehemiah Antoine was supported by the Tom Rybolt and Richard X. Zhang Endowed Undergraduate Research in Chemistry Scholarship. Marisa James was supported by the William H. Wheeler Center for Odor Research.

References

[1] Das, P. *et al.* (2014) S. Synthesis, Crystal Structure, DNA Interaction and in Vitro Anticancer Activity of a Cu(II) Complex of Purpurin: Dual Poison for Human DNA Topoisomerase I and II. *RSC Adv.* 4 (103), 59344–59357.

[2] Dumele, O. *et al.* (2014) Halogen Bonding of (Iodoethynyl)Benzene Derivatives in Solution. *Organic Letters*. 16 (18), 4722–4725.

[3] Tse, Y. C. *et al.* (2021) Lithium Halide Ion-Pair Recognition with Halogen Bonding and Chalcogen Bonding Heteroditopic Macrocycles. *Chemical Communications*. 57 (40), 4950–4953.

[4] Yan, X. *et al.* (2023) 2D Organic Materials: Status and Challenges. *Advanced Science.* 10 (7), 2203889.

Figures

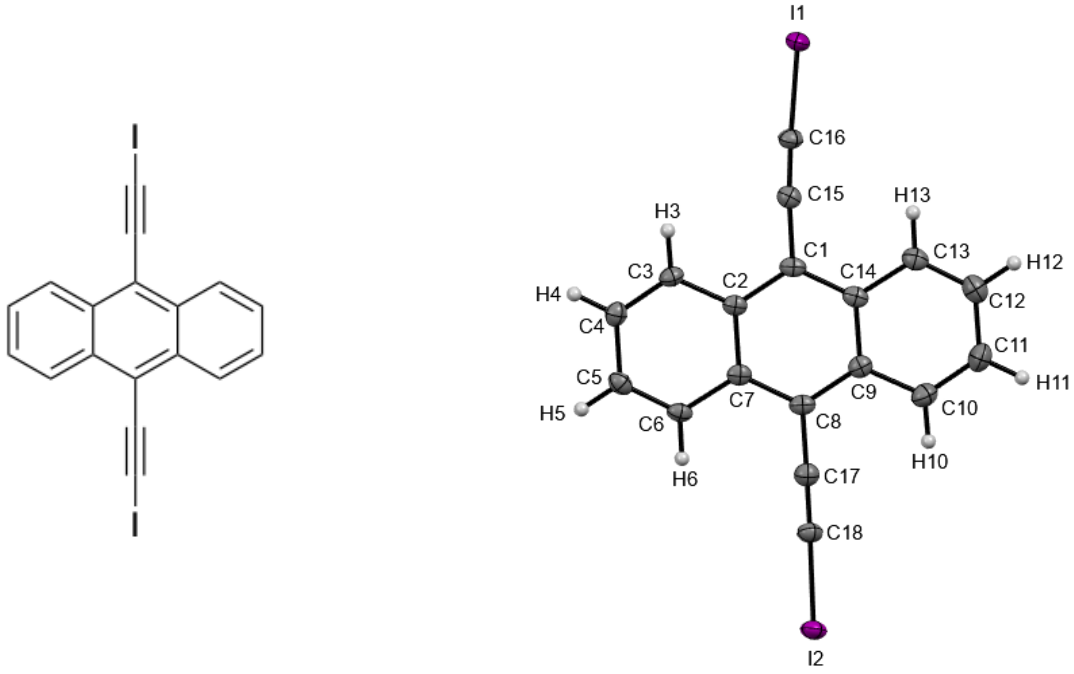

Figure I: 9,10-Bis-(iodoethynyl)anthracene's skeletal structure (left) and crystal structure (right). All atoms are labeled for context for Tables III and IV.

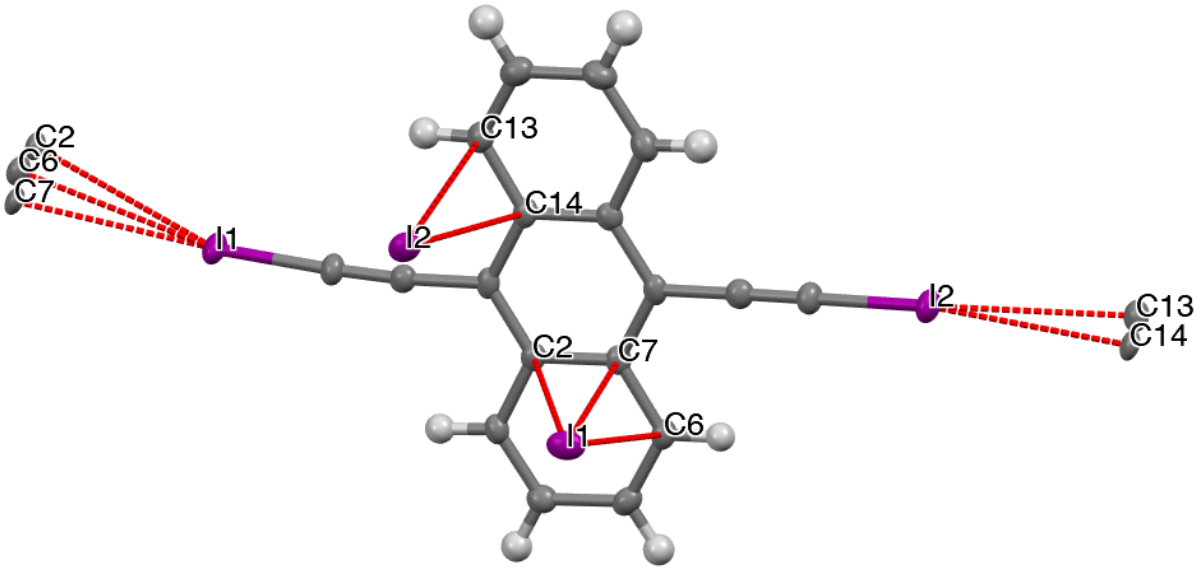

Figure II: A depiction of the I-π interactions (shown in red) that occur in the crystal of the title compound. I1 does three halogen bonds, and I2 does two.

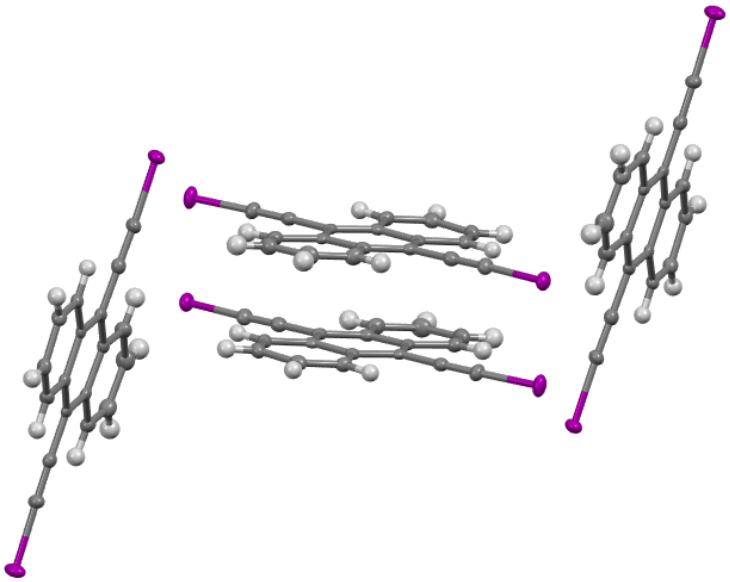

Figure III: A closer view of the π-π stacking between adjacent moieties of the title compound.